GAS DISCHARGE MODES AT A SINGLE NOZZLE IN TWO-DIMENSIONAL FLUIDIZED BEDS

CHENG-CHUNG HUANG AND CHIEN-SONG CHYANG
Chemical Engineering Department, Chung Yuan Christian University, Chung Li, Taiwan, R.O.C.

Key Words: Fluidized Bed, Bubbling, Jetting, Spouting, Pressure Fluctuations

Bubbling, jetting and spouting as gas discharge modes at a single nozzle in a two-dimensional gas-fluidized bed with Group B particles were investigated by means of visual observation and spectral analysis of pressure fluctuations in the grid region. A bubble plume was observed with a frequency of bubble formation in the range 2–7 Hz. Empirical equations predicting the transitions of gas discharge modes were obtained. The flow regimes of gas discharge modes were mapped by using two parameters, the static bed height-to-nozzle diameter ratio and a modified two-phase Froude number.

Introduction

It is well known that the grid region in a gas-fluidized bed reactor plays an important role in determining the chemical conversion, especially for a fast reaction, and the efficiencies of some physical operations. When the fluidizing gas flows through a multiorifice distributor into a fluidized bed, it can form bubble plumes, pulsating jets or spouts at the orifices. Pulsating jets and spouts can be regarded as permanent jets.[4] The gas discharge modes at the orifices significantly affect the hydrodynamics in the grid region. Eventually, the gas discharge modes affect the gas-solids contacting as well as the heat and mass transfer processes; therefore, reasearch concerning the gas discharge modes at the orifices is very important.

Generally speaking, for a given system a bubble plume forms at an orifice at low gas velocities but a pulsating jet or spout forms at high gas velocities.[6] Rowe *et al.*[12] observed that a bubble plume, rather than a permanent jet, was a more typical mode of gas discharge at an orifice. The same result was reported in subsequent works.[18,19] A permanent jet may appear at an orifice when particles around the orifice are not well fluidized or the flow of solids towards the orifice is hindered by surfaces.[10,12,16] A jet can be stablized by increasing the particle size, gas velocity through an orifice, and gas to solid density ratio,[2,8,17] or decreasing the ratio of bed height to orifice diameter.[9] In a bed equipped with a multiorifice distributor, Wen *et al.*[16] found that jetting will transit to bubbling while the gas velocity is increased to a certain value which is high enough to diminish the dead zones of solids between orifices. Yates *et al.*[20] suggested that a jet can be observed if the void height above an orifice is greater than the radius of the initial bubble. The validity of this criterion was not verified. The criterion $d_o/d_p \leqslant 25.4$ proposed by Chandnani and Epstein[1] for stable spouting was shown by Grace and Lim[4] to give a good separation between gas-solid systems that form permanent jets and those that form bubble plumes. However, it is over simplified because the effects of several important factors such as jet momentum, particle and gas density, and bed height are not taken into account. Massimilla[9] has made an extensive review of works on the study of jets. Experimental work on the transition from one gas discharge mode to another at an orifice is still sparse.

Spectral analysis of pressure fluctuation signals has been widely used to investigate the bubbling dynamics in a gas-fluidized bed. Recently, this technique was applied in the study of the gas discharge modes at an orifice.[3,7,15] Zhang *et al.*[21] investigated jet instability and bubble formation above a single orifice in a two-dimensional bed by analyzing the fluctuation signals measured by a capacitance probe.

In this work, spectral analysis of pressure fluctuations in the grid region was used to investigate the effects of nozzle diameter, gas velocity through the nozzle, particle size and static bed height on the gas discharge modes at a single nozzle in a two-dimensional bed. We attempted to find empirical equations for predicting the transitions from one mode to another and to map the flow regimes of gas discharge modes.

1. Experimental

A schematic diagram of the experimental apparatus is shown in **Fig. 1**. All the experiments were conducted in a two-dimensional fluidized bed fabricated of acrylic

* Received March 1, 1991. Correspondence concerning this article should be addressed to C. S. Chyang.

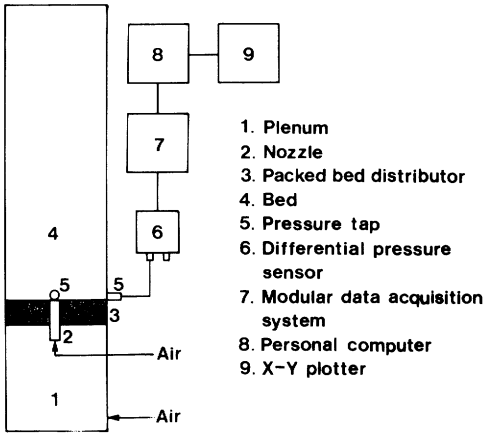

Fig. 1. Schematic diagram of the experimental apparatus

plates. The cross section of this bed was 400 mm × 15 mm. The bed materials tested were glass beads of Group B particles with mean diameters of 214, 359 and 545 μm. A single nozzle mounted flush with a packed-bed distributor was used to inject an independent air flow into the bed. The inside diameters of the nozzles tested were 3.2, 6.0 and 8.44 mm. The gas velocity through the nozzle was in the range 1 to 120 m/s. In the packed-bed distributor, glass beads with a mean diameter of 214 μm were packed between a 200-mesh screen and a bottom perforated plate covered with a screen. The primary fluidizing air through the packed-bed distributor was kept at the minimum fluidization velocity of the bed material. This means that the gas flow through the nozzle into the bed can theoretically form a complete jet, a bubble plume or a spout. In a practical gas-fluidized bed the dense phase is usually regarded as the status of minimum fluidization. If the primary fluidizing gas and the gas injected through the nozzle are independently supplied, the respective effects of gas momentum at the nozzle and the fluidization status on the gas discharge modes can be identified. All the experimental conditions are listed in **Table 1**.

Two pressure taps, mounted flush with the wall at a height 15 mm from the distributor, were used to measure the pressure fluctuations in the grid region. One was located at the nozzle axis of the front wall. The other was located on the side wall. The inside opening of the tap was covered with a 200-mesh screen to prevent solids from entering the tap. The data acquisition system consisted of a SenSym SCX01DNC differential-pressure sensor with two input channels, an ACUREX 7000-MDAS modular data acquisition system and a personal computer. The operating pressure of the differential pressure sensor is 0 to 6.9 kPa. The accuracy is $\pm 0.2\%$ of the full-scale span output. The 7000-MDAS executed the acquisition of pressure fluctuation signals and fast Fourier transform of the time domain data to obtain the frequency

Table 1. Experimental conditions

Bed cross section (mm × mm)	400 × 15
Distributor	Packed-bed distributor
Nozzle diameter (mm)	3.2, 6.0, 8.44
Particle	Glass beads
Average particle size (μm)	214, 359, 545
Minimum fluidization velocity	0.048, 0.074, 0.186
Velocity through nozzle (m/s)	1–120
Velocity through distributor (m/s)	Minimum fluidization velocity
Static bed height (m)	0.05, 0.1, 0.15, 0.2, 0.3

domain data. The personal computer was used to control the 7000-MDAS for implementing the sampling and spectral analysis of pressure fluctuation signals.

In each test run the gas flow through the nozzle was first increased sharply till a pulsating jet could be observed at the nozzle. Then it was further decreased or increased to the required flow rate. The gas discharge mode was observed from the transparent wall. The high-pressure input of the differential-pressure sensor was connected to the front-wall or side-wall pressure tap. The low-pressure input was exposed to the atmosphere. The output signal of the differential-pressure sensor was transmitted to the 7000-MDAS for spectral analysis. The sampling interval of the pressure fluctuations was 25 ms. For each test 10 × 512 points were sampled and processed. The total sampling time was 128 seconds. The mean amplitude of pressure fluctuations was calculated by the following equation, as reported by Svoboda *et al.*[13] and Puncochar *et al.*[11]

$$Y=\left\{\frac{1}{N-1}\sum_{i=1}^{N}(P_i-\bar{P})^2\right\}^{1/2} \tag{1}$$

where N is the total number of sampled points and P_i is the instantaneous value of each point. The mean pressure, $\bar{P}$, is calculated by

$$\bar{P}=\frac{1}{N}\sum_{i=1}^{N}P_i \tag{2}$$

2. Results and Discussion

In this study, a bubble plume could be observed at the nozzle for some specific operating conditions, especially at low gas velocities through the nozzle and at low bed heights. A typical pulsating jet could be clearly observed at higher gas velocities in a deeper bed of larger particles. The initial bubble formed and detached at the end of the jet. As the jet penetrated the bed surface, a steady spout formed and a significant fountain was observed. As shown in **Fig. 2**, the power spectral densities of pressure fluctuations corresponding to these three typical modes all reveal a major frequency. It also indicates that for each mode the power spectral density of pressure fluctuations

measured at the nozzle is higher than that measured at the side-wall tap, but the major frequencies are the same. From all the results of this study for the jetting mode, it was found that the difference between the power spectral density of pressure fluctuations measured at the nozzle and that measured at the side-wall tap decreased as the stability of the jet increased. For a bubbling mode, the power spectral density of pressure fluctuations measured at the nozzle was much higher than that measured at the side-wall tap. As to a typical spouting mode, a sharp peak of the power spectral density measured at the nozzle which gave a major frequency higher than 5 Hz, and a very low power spectral density measured at the side wall tap were found.

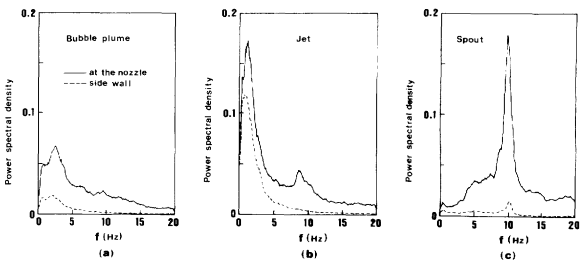

Fig. 2. Power spectral density of pressure fluctuations corresponding to a bubble plume, a jet and a spout.
(a) $d_p=214\,\mu m$, $d_o=6\,mm$, $H_s=0.15\,m$, $U_0=5.7\,m/s$
(b) $d_p=545\,\mu m$, $d_o=8.44\,mm$, $H_s=0.3\,m$, $U_o=17.2\,m/s$
(c) $d_p=214\,\mu m$, $d_0=6\,mm$, $H_s=0.1\,m$, $U_o=34\,m/s$

Table 2 shows the specific experimental conditions which resulted in a bubbling mode. It indicates that the major frequency is in the range 2 to 7 Hz. This is consistent with the results of Filla *et al.*[3] obtained in a two-dimensional bed. For a three-dimensional bed, the frequency of bubble formation at a single nozzle has been reported as 18–21 Hz,[5] 19–25 Hz[6] and 6–8 Hz.[12,14,19] In **Table 3** we list experimental conditions in the literature which resulted in the bubbling of gas at a nozzle or an orifice. The reason why there are significant discrepancies in these data

Table 2. Major frequency of pressure fluctuations for the mode of a bubble plume

d_p (μm)	d_o (mm)	H_s (m)	U_o (m/s)	Major frequency (Hz)
214	3.2	0.1	5.3	2.7
	6	0.1	1.1	2.8
	6	0.1	5.7	5.7
	6	0.15	5.7	2.4
	6	0.2	5.7	2.13
359	6	0.05	1.2	6.5
	8.44	0.05	1.2	6.4
	8.44	0.1	1.2	1.9
545	6	0.05	1.14	2.0
	6	0.1	5.7	2.4
	6	0.1	11.3	3.6
	8.44	0.05	1.2	5.85

Table 3. Experimental conditions in the literature and this work concerning bubble formation at an orifice

Investigators	Bed scale (m)	Gas disch. config.	Particles	Part. dia. (mm)	Density (kg/m^3)	Nozzle dia. (mm)	Static bed height (m)	Background gas (m/s)	Nozzle gas velocity (m/s)
Harison and Leung (1961)	0.152 dia.	1	Sand	0.152*	2640	1.25–9.4	0.18–0.35	U_{mf}–$1.66U_{mf}$	0.81–24.5
			Alumina cat.	0.05*	2040				
	0.61 × 0.61	1	Sand	0.152*	2640	25.4	0.324	U_{mf}–$1.5U_{mf}$	0.3–15.8
Hsiung and Grace (1978)	0.08 × 0.1	1	GB	0.107–0.335*	2500*	1.6–6.3	0.03	$1.15U_{mf}$	0.6–60
Rowe *et al.* (1979)	0.14 dia., 0.152 dia.	1	Alumina	0.15	2700*	6.4–15.9	0.15, 0.3	U_{mf}	1–70
			Sand	0.2	2600*				
			Catalyst	0.052	—				
			Mineral	0.2	—				
Yates *et al.* (1984)	0.2 × 0.3	1	Alumina	<0.15, 0.3*	2700*	10	—	U_{mf}	0.85–26.75
Filla *et al.* (1986)	0.39 × 0.016	1	Sand	0.3*	2500	6	0.11–0.31	$7.8U_{mf}$	30
This work	0.4 × 0.015	1	GB	0.214–0.545	2500	3.2–8.44	0.05–0.15	U_{mf}	1.1–11.3
Sit and Crace (1986)	0.152 dia. (Half column)	2	GB	0.12–0.31	2500	6.4	0.28–0.3	U_{mf}	10–50
			Copolymer	0.29	1100				
Oki *et al.* (1980)	0.28 dia.	3	GB	0.221	2500*	5	0.2 (H_{mf})	$1.5U_{mf}$–$8U_{mf}$	15.8–78
Yang *et al.* (1984)	0.113 dia.	3	Catalyst	—	—	3.8–10	—	$6U_{mf}$–$20U_{mf}$	$769U_{mf}$–$2564U_{mf}$

1: A single nozzle was mounted flush with a porous plate. A filter cloth distributor was used by Harrison and Leung (1961).
2: A single nozzle was mounted flush with a perforated plate.
3: Perforated plate only.
*: Estimated.

of bubble formation frequencies is not clear. The difference in techniques used to detect bubble formation may be one of the causes. The bed height tested by Hsiung and Grace[6] was so low that the fluctuations in bed height might affect the fluctuation signals at the nozzle. In the paper of Harrison and Leung,[5] whether a bubble formed right at the orifice or at the end of a jet was not clearly stated.

When the gas velocity through the nozzle is increased from zero, the gas discharge mode was observed to change from a quiescent bed to bubbling, jetting to spouting. **Figure 3** shows the variation of power spectral density of pressure fluctuations with the gas velocity through the nozzle. According to the procedure for adjusting the gas velocity through the nozzle mentioned above, a very small permanent void was found immediately above the nozzle at the velocity 1.1 m/s. There was no solid motion near and above the void; therefore, the bed could be regarded as a quiescent bed. One has to note that the solids in a quiescent bed in this study were at the minimum fluidization status. The corresponding power spectral density of pressure fluctuations measured at the nozzle is very small but has a high major frequency of 15.3 Hz. The power spectral density detected at the side wall is nearly zero. The bubbling and jetting modes alternately appeared when the gas velocity was in the range 1.1 to 22.8 m/s. The typical jetting mode did not appear until 22.8 m/s. At 34.1 m/s, jetting and spouting alternately appeared but jetting was still the dominant mode. The corresponding power spectral density of pressure fluctuations shows that the major and minor frequencies are 3 and 8 Hz, respectively. As the gas velocity increased to 45.4 m/s, spouting became the dominant mode so that the major frequency is 8 Hz and the minor frequency 3 Hz. A steady spout was observed when the gas velocity was higher than 50 m/s, and a similar power spectral density distribution as shown in Fig. 2(c) was obtained. Visual observation coupled with the results shown in Fig. 3 indicate that the transition from one mode to another is a continuous process, i.e., the transition process occurred in a range of gas velocities through the nozzle. A similar observation concerning with the transition from bubbling to jetting was reported by Rowe *et al.*[12] In the case shown in Fig. 3, the transition process from jetting to spouting is noted by the appearance of a significant minor frequency of pressure fluctuations.

Figure 4 shows the typical effect of gas velocity through the nozzle on the major frequency. The major frequencies of a quiescent bed with a small permanent void at the nozzle are not included in this figure. The curves generally show a sharp increase in the major frequency followed by a shoulder. Based on visual observation and the results shown in Fig. 3,

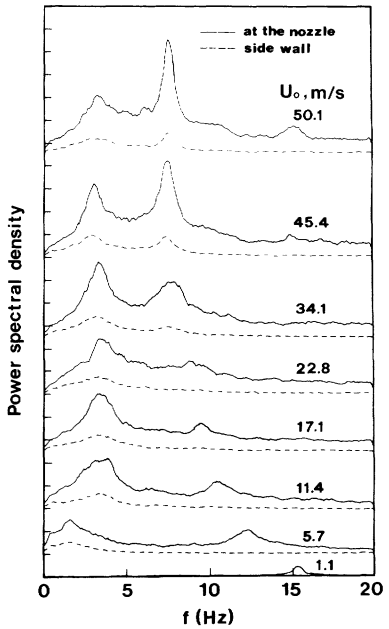

Fig. 3. Variation of power spectral density of pressure fluctuations with gas velocity through the nozzle. $d_p = 359\ \mu m$, $d_o = 6$ mm, $H_s = 0.15$ m

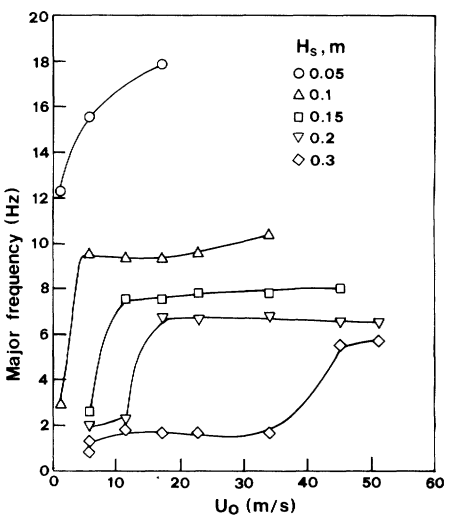

Fig. 4. Effect of gas velocity through the nozzle on the major frequency of pressure fluctuations. $d_p = 214\ \mu m$, $d_o = 8.44$ mm

we note that the transition process from jetting to spouting gave a major and a minor frequency. It is probable that the point at the shoulder was in the transition process with a significant minor frequency. Even when spouting was the dominant mode, jetting or bubbling appeared frequently. Thus, the shoulder of each curve shown in Fig. 4 could not exactly represent the transition point. When the static bed height was greater than 0.1 m, the major frequency tended to level off after the shoulder for all the particles tested. It also can be found from Fig. 4 that the major frequency of a spouting mode decreases as static bed height increases.

The effect of gas velocity through the nozzle on the mean amplitude of pressure fluctuations at the nozzle corresponding to Fig. 4 is shown in **Fig. 5**. As long as a spout could form, a peak of the curve could be found. The decrease in mean amplitude with gas velocity after the maximum point implies that the mode has completely transited from jetting or bubbling to spouting. Compared to the results shown in Fig. 4, the maximum points of the curves shown in Fig. 5 could be defined as the transition points from bubbling or jetting to spouting. As a matter of fact, the gas velocities corresponding to the maximum points shown in Fig. 5 were usually greater than those corresponding to the shoulders shown in Fig. 4.

At a given gas velocity through the nozzle the gas discharge mode was found to transit from spouting to jetting or bubbling, and then to a quiescent bed as the static bed height increased. **Figure 6** shows the effect of static bed height on the major frequency of pressure fluctuations for 545 μm glass beads. As mentioned above, there was a small permanent void at the nozzle in a quiescent bed. There was no solid motion near and above the void. No significant pressure fluctuations were found. This resulted in a very small power spectral density but with a high major frequency. The gas injected through the nozzle flowed into the dense phase through the boundary of the small permanent void. The high major frequency but very low power spectral density of the pressure fluctuations measured at the orifice represented the characteristics of gas flow through such a path. Except for 120 m/s, the major frequency significantly decreases to a minimum of about 0.4 Hz and then sharply increases as the static bed height increases. When jetting or bubbling occurred at low gas velocities the major frequencies were usually found to be about 0.4 Hz. Therefore, the minimum points of the curves in Fig. 6 could not exactly represent the transitions from jetting or bubbling to a quiescent bed.

Figure 7 illustrates the typical effect of static bed height on the mean amplitude of pressure fluctuations at the nozzle corresponding to the data of major frequency shown in Fig. 6. An increase in static bed height would destablize the spouting and made it transit to jetting or bubbling. This resulted in the first increase in mean amplitude. If the gas velocity through the nozzle was not high enough, further increase of the static bed height would result in a quiescent bed and consequently a decrease of the mean amplitude was found. The reproductivity of the data shown in Figs. 6 and 7 was quite good. Compared to the results shown in Fig. 6, the maximum point of each curve in Fig. 7 could be defined as the transition point from a quiescent bed to a bed with jetting or bubbling of gas at the nozzle.

From Figs. 6 and 7, it is found that the results

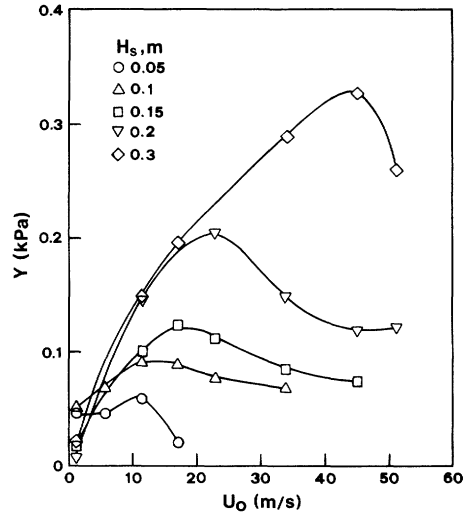

Fig. 5. Effect of gas velocity through the nozzle on the mean amplitude of pressure fluctuations at the nozzle. $d_p = 214\ \mu$m, $d_o = 8.44$ mm

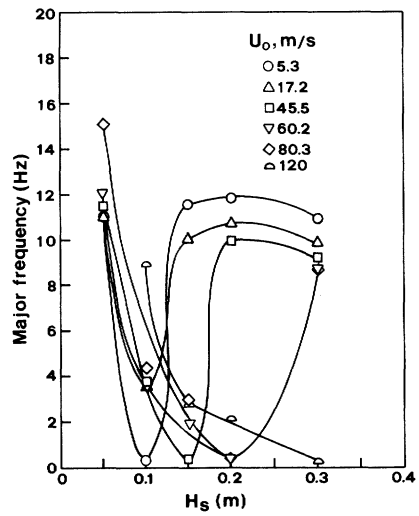

Fig. 6. Effect of static bed height on the major frequency of pressure fluctuations. $d_p = 545\ \mu$m, $d_o = 3.2$ mm

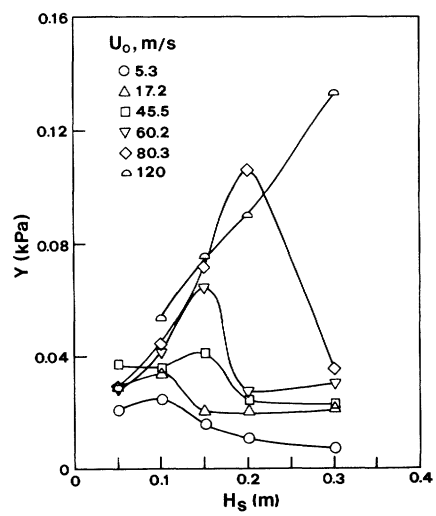

Fig. 7. Effect of static bed height on the mean amplitude of pressure fluctuations at the nozzle. $d_p = 545\ \mu$m, $d_o = 3.2$ mm

obtained at $U_o = 120$ m/s were quite different from those in the other cases where a quiescent bed with a permanent void eventually resulted when the static bed height increased to 0.3 m. This is because the gas velocity through the nozzle was so high that a quiescent bed could no longer result. The mode transited from spouting to steady jetting as the static bed height increased from 0.1 to 0.3 m. Thus the major frequency was found to decrease with static bed height. At a higher static bed height, jet bubbles grew to a larger size; therefore, the mean amplitude increased with static bed height.

To take account of the effects of particle size, nozzle diameter, static bed height and gas velocity through the nozzle on the gas discharge modes, we used two parameters to map the flow regimes. They are the ratio of static bed height to nozzle diameter and a modified two-phase Froude number. The latter was defined as

$$Fr^* = \left(\frac{\rho_f}{\rho_p - \rho_f} \frac{U_o^2}{g d_p} \right)^{1/2} \tag{3}$$

It represents the balance between the inertial force of gas at the nozzle and the gravitational force of the bed. Based on the transition points defined by the results shown in Figs. 5 and 7 for all the particles and experimental conditions tested, the transition from a quiescent bed to bubbling or jetting can be represented by Eq. (4).

$$H_s/d_o = 21.9 \exp(0.076 Fr^*) \tag{4}$$

The standard deviation of Eq. (4) is 16.9%. The transition from bubbling or jetting to spouting can be represented by Eq. (5).

$$H_s/d_0 = 3.56 (Fr^*)^{0.68} \tag{5}$$

The standard deviation of Eq. (5) is 25.7%.

Figure 8 shows the flow regimes of gas discharge modes at a single orifice. It also includes the data in the literature which provided sufficient experimental conditions and resulted in the bubbling mode at the orifice. The transition from bubbling to jetting could not be efficiently defined by the spectral analysis of pressure fluctuations at the single nozzle. Based on the data shown in Fig. 8, a transition criterion, $H_s/d_o = 23.1$, was proposed. It is represented by the dotted line. Thus, the criterion for jetting mode at a single nozzle is

$$H_s/d_o > 23.1 \tag{6a}$$

and

$$3.56 (Fr^*)^{0.68} < H_s/d_o < 21.9 \exp(0.076 Fr^*) \tag{6b}$$

In Fig. 8, it is found that the data of Sit and Grace[14] are located in the region of the jetting mode. In their study, the assumption of the formation of a bubble right at an orifice gave a good interpretation about

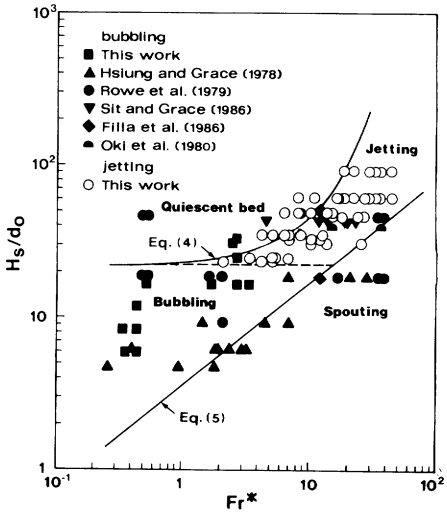

Fig. 8. Flow regimes of gas discharge mode at a single nozzle

the data of interphase mass transfer; however, the bubbling mode at the orifice could not be verified by the flow visualization carried out in a half-column. As shown in Fig. 2 of their paper, a pulsating jet was a more typical mode of gas discharge at the orifice for the conditions they tested. The data of Filla *et al.*[3] and Oki *et al.*[10] are located in the region of the jetting mode. In Table 3, one can see that the background gas velocities they used were much higher than the minimum fluidization velocity. This may be the main reason why the flow regimes map presented in this work cannot fit their data. The bed height tested by Hsiung and Grace[6] was only 0.03 m. They observed that no jets broke the bed surface for the conditions studied. Figure 8 shows that most of their data appear near the margin between the bubbling mode and the spouting mode.

Figure 8 also shows that some data of Rowe *et al.*[12] appear in regions other than the region of the bubbling mode. The gas velocities through the nozzle presented in their paper, which resulted in the bubbling mode, were less than 30 m/s. They stated that they applied their observations over the full range of conditions they tested. Besides the data clearly presented in their paper, for beds of alumina and sand at a bed height of 0.3 m the inferred data based on the two end-points of the range of gas velocity through the nozzle shown in Table 3 are also plotted in Fig. 8. It is found that the flow regimes map can fairly fit the data which were clearly presented in their paper; however, it cannot fit the inferred data. There are two inferred data points in each of the three regions: quiescent bed, jetting, and spouting mode.

The data of Harrison and Leung[5] are not shown in Fig. 8 because the mechanism of bubble formation was not verified in their paper. They used capacitance probes to measure the fluctuation signals for bubble formation at an orifice in a three-dimensional bed,

and the bubble frequency was estimated from the fluctuation signals. Whether the bubble released right from the orifice or from the end of a jet was ambiguous. According to the comparison shown in Table 3 and Fig. 8, our data are applicable to three-dimensional cases. To date, however, data concerning the transitions from one mode to another are limited. More data obtained by other investigators in the future are necessary to verify our criteria.

The results obtained in this work and the available bubbling-mode data in the literature are for Geldart B group particles. Caution should be taken when applying the results obtained in this work to Geldart A group particles. Further investigation and verification are required. In the flow regimes map of the gas discharge modes at a single nozzle presented in this study, we did not consider the interaction of gas issuing from adjacent orifices of a multiorifice plate. The fluidization status of solids surrounding the orifice would also be an important factor in the gas discharge modes. These will be the main topics of our further study.

Conclusion

Spectral analysis of pressure fluctuations was used to investigate the transitions of gas discharge modes at a single nozzle in a two-dimensional bed. The power spectral density measured at the nozzle was higher than that measured at the side wall, but the same major frequency was obtained. A bubble plume was observed in the two-dimensional bed with a frequency of bubble formation in the range 2–7 Hz.

The appearance of a minor frequency of the power spectral density distribution characterized the transition process from bubbling or jetting to spouting. From the spectral analysis of pressure fluctuations the transition point from a quiescent bed to bubbling or jetting mode and that from bubbling or jetting to spouting mode can be defined. The flow regimes of gas discharge modes were mapped by using two parameters, the ratio of static bed height to nozzle diameter and a modified two-phase Froude number. An empirical criterion for the transition from bubbling mode to jetting mode was proposed.

Acknowledgement

The authors wish to thank the National Science Council, R.O.C., for financial support under Grant No. NSC78-0402-E033-02.

Nomenclature

d_p	=	particle diameter	[m]
d_0	=	nozzle diameter	[m]
Fr^*	=	modified two-phase Froude number, $\left(\frac{\rho_f}{\rho_p-\rho_f}\frac{U_o^2}{gd_p}\right)^{1/2}$	[—]
f	=	frequency	[Hz]
H_s	=	static bed height	[m]
N	=	total number of sampled points	[—]
$\bar{P}$	=	mean pressure	[kPa]
P_i	=	instantaneous pressure	[kPa]
U_o	=	gas velocity through the nozzle	[m/s]
Y	=	mean amplitude of pressure fluctuations	[kPa]
ρ_f	=	density of fluid	[kg/m^3]
ρ_p	=	density of particle	[kg/m^3]

Literature Cited

1) Chandnani, P. P. and N. Epstein: "Fluidization V", K. Ostergaard and A. Sorensen, Eds., Engineering Foundation, New York, p. 233 (1986).
2) Donsi, G., L. Massimilla and L. Colantuoni: "Fluidization", J. R. Grace and J. M. Matsen, Eds., Plenum Press, New York, p. 297 (1980).
3) Filla, M., L. Massimilla, D. Musmarra and S. Vaccaro: "Fluidization V ", K. Ostergaard and A. Sorenson, Eds., Engineering Foundation, New York, p. 71 (1986).
4) Grace, J. R. and C. J. Lim: *Can. J. Chem. Eng.*, **65**, 160 (1987).
5) Harrison, D. and L. S. Leung: *Trans. Instn. Chem. Engrs.*, **39**, 409 (1961).
6) Hsiung, T. P. and J. R. Grace: "Fluidization", J. F. Davidson and K. L. Keairns, Eds., Cambridge University Press, p. 19 (1978).
7) Huang, C. C. and C. S. Chyang: "Fluidized-Bed & Three-Phase Reactors", W. M. Lu and L. P. Leu, Eds., Kenting, Taiwan, p. 9 (1990).
8) Knowlton, T. M. and I. Hirsan: "Fluidization", J. R. Grace and J. M. Matsen, Eds., Plenum Press, New York, p. 315 (1980).
9) Massimilla, L.: "Fluidization", J. F. Davidson, R. Clift and D. Harrison, Eds., Academic Press, London, Chapter 4, p. 133 (1985).
10) Oki, K., M. Ishida and T. Shirai: "Fluidization", J. R. Grace and J. M. Matsen, Eds., Plenum Press, New York, p. 421 (1980).
11) Puncochar, M., J. Drahos, J. Cermak and K. Selucky: *Chem. Eng. Commun.*, **35**, 81 (1985).
12) Rowe, P. N., H. J. MacGillivray and D. J. Cheesman: *Trans. Instn. Chem. Engrs.*, **57**, 194 (1979).
13) Svoboda, K., J. Cermak, M. Hartman, J. Drahos and K. Selucky: *Ind. Eng. Chem. Process Des. Dev.*, **22**, 514 (1983).
14) Sit, S. P. and J. R. Grace: "Fluidization V", K. Ostergaard and A. Sorenson, Eds., Engineering Foundation, New York, p. 39 (1986).
15) Vaccaro, S., D. Musmarra, F. Costanza, M. Filla and L. Massimilla: "Fluidization VI", J. R. Grace, L. W. Shemilt and M. A. Bergougnou, Eds., Engineering Foundation, New York, p. 245 (1989).
16) Wen, C. Y., N. R. Deale and L. H. Chen: *Powder Technol.*, **31**, 175 (1982).
17) Yang, W. C. and D. L. Keairns: *AIChE Symp. Ser.*, **70**(141), 27 (1974).
18) Yang, X. T., D. G. Horne, J. G. Yates and P. N. Rowe: *AIChE Symp. Ser.*, **80**(241), 41 (1984).
19) Yates, J. G., P. N. Rowe and D. J. Cheesman: *AIChE J.*, **30**, 890 (1984).
20) Yates, J. G., V. Bejcek and D. J. Cheesman: "Fluidization V", K. Ostergaard and A. Sorenson, Eds., Engineering Foundation, New York, p. 79 (1986).
21) Zhang, X. R., G. M. Homsy and W. T. Ropchan: *Int. J. Multiphase Flow*, **13**(5), 649 (1987).